

Interfacial barrier in manganite junctions with different crystallographic orientations

W. W. Gao, A. D. Wei, J. R. Sun,^{a)} D. S. Shang, J. Wang, T. Y. Zhao, and B. G. Shen
Beijing National Laboratory for Condensed Matter Physics and Institute of Physics, Chinese Academy of Sciences, Beijing 100190, People's Republic of China

(Received 9 April 2010; accepted 18 May 2010; published online 28 June 2010)

We performed a comprehensive study on the $\text{La}_{1-x}\text{Ca}_x\text{MnO}_3/\text{SrTiO}_3:\text{Nb}$ junctions with different hole content and film thickness. It is found that the interfacial barrier, which determines the physical properties of the junctions, shows a strong dependence on crystallographic orientation, and it is substantially higher for the (110) than for the (100)-orientated junctions. The difference in barrier height is further found to exhibit a systematic variation with Ca content and film thickness (t). It reduces from ~ 0.09 to 0.02 eV for a x increase from 0.1 to 1 with a fixed $t=200$ nm, and experiences a growth by ~ 0.06 eV corresponding to the variation in t from 10 to 160 nm for a constant $x=0.33$. Similar phenomena have been observed in the $\text{La}_{0.67}\text{Ba}_{0.33}\text{MnO}_3/\text{SrTiO}_3:\text{Nb}$ junctions. In the scenario of different polarity mismatches at the (100) and (110) interfaces in the two series of junctions, these results can be qualitatively understood. © 2010 American Institute of Physics. [doi:10.1063/1.3447797]

Manganite-based heterojunction is a typical example of doped Mott insulators. It exhibits diverse features that are absent in conventional junctions, such as magnetic field-dependent rectifying characteristics and photovoltaic effects.¹⁻³ As well established, the properties of the manganite junction is exclusively determined by interfacial barrier (IB) which is sensitive to interface state, both structural and electronic states. There are intensive efforts to adjust the rectifying behaviors of the junction by modifying interface, for the purpose of either fundamental research or practical application. It has been found that the tensile stress in the manganite film, imposed by substrate, can cause an obvious decrease in the height of the IB.⁴ An intermediate layer with a thickness a few unit cells is also found to significantly affect the IB.⁵ Particularly, even the crystallographic orientation of the substrate has a strong effect, and a reduction of ~ 0.1 eV in the IB height can be resulted when the film plane changes from (100) to (110).⁶

These results are interesting in a sense that they demonstrate the great potential of the structural degree of freedom at the interfaces in modifying perovskite heterojunctions. However, work on the influence of interfacial structure is very limited at present, sometimes only special cases are considered. For example, the $\text{SrTiO}_3:\text{Nb}$ substrates involved in the junction previously studied have been processed at high temperature in high vacuum.⁶ This may cause an aggregation of the Nb atoms on the surface of the substrate, thus an unusual junction interface. Moreover, the manganite has a constant Sr content of 0.4. Different hole content may lead to different interface states, thus different orientation dependences. Based on these considerations, in this letter we have performed a comprehensive study on the effect of crystallographic orientation for the $\text{La}_{1-x}\text{Ca}_x\text{MnO}_3/\text{SrTiO}_3:\text{Nb}$ (LCMO/STON) junction with a Ca content between 0 and 1. The IB is found to show a strong dependence on crystallographic orientation, and it is substantially higher for

the (110) than for the (100)-orientated junctions. A systematic variation in the barrier difference with the hole content (x) and film thickness (t) of the LCMO is further detected. Similar behaviors are observed in the $\text{La}_{0.67}\text{Ba}_{0.33}\text{MnO}_3/\text{SrTiO}_3:\text{Nb}$ (LBMO/STON) junctions.

LCMO-based junctions were fabricated by growing, via the pulsed laser ablation technique, LCMO films with the Ca content of 0, 0.1, 0.2, 0.33, 0.67, 0.75, and 1 on the (001) and (110)-orientated STON substrates, respectively. During the deposition, the temperature of the substrate was kept at 720 °C, and the oxygen pressure at 10 Pa, for $x=0$, 30 Pa, for $x=0.1$, 50 Pa, for $x=0.2$, and 80 Pa, for $x \geq 0.33$. The film thickness is $t \sim 200$ nm, controlled by deposition time. For the optimal doping level $x=0.33$, two series of junctions with the film thickness ranging from $t=5$ nm to 200 nm were further prepared, respectively, on two kinds of substrates. For a comparison study, the LBMO/STON junctions with different film thickness were also prepared.

The lateral size of the junction is 1×1 mm², fabricated by the photolithographic and chemical etching technique. As electrodes, two copper pads were deposited on LCMO (LBMO) and STON, respectively, and the contact resistance is ~ 15 Ω for the Cu-STON contact and ~ 200 Ω for the Cu-LCMO (LBMO) contact. Lasers with a wavelength between 532 and 980 nm were used in the present experiments. The spot size of the laser is ~ 1 mm in diameter. Photocurrent, I_p , yielded by laser illumination was acquired at the ambient temperature by a Keithley 2611 SourceMeter.

As expected, I_p exhibits a strong dependence on photon energy, and the typical value for the (100) LCMO/STON junction of $x=0.33$ and $t=160$ nm is ~ 42.5 nA/mW for a laser of 532 nm and ~ 9.5 nA/mW for a laser of 780 nm. In contrast, the photovoltaic effect in LBMO/STON is much strong, and the corresponding photocurrents are ~ 195.7 and 25.3 nA/mW. Probably due to the variation in diffusion length of the excited charge carriers, the photocurrent for a fixed wavelength of, for example, 532 nm, shows a remarkable dependence on Ca content, decreasing from ~ 72.9 to 0.8 nA/mW as x grows from 0.1 to 1.

^{a)} Author to whom correspondence should be addressed. Electronic mail: jrsun@g203.iphy.ac.cn.

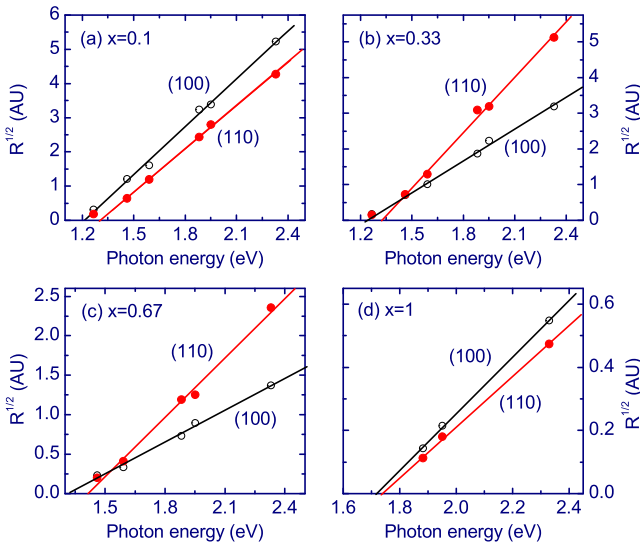


FIG. 1. (Color online) Square-root quantum efficiency as a function of photon energy for the (100) and (110)-orientated LCMO/STON junctions with different Ca content and a constant film thickness of 200 nm. Solid lines are fitting results.

As well established, the information about the IB can be extracted from the internal photoemission spectra. According to Fowler,⁷ there is a simple relation between the quantum efficiency R of the photoemission process, proportional to the photocurrent yielded by each photon, and photon energy: $R \propto (h\nu - \Phi_B)^2$ if $E_F \gg |h\nu - \Phi_B| \gg 3k_B T$, where $h\nu$ is the photon energy and Φ_B the height of the IB. A direct calculation shows that the depletion layer mainly develops in STON. As a result, LCMO(LBMO)/STON can be well approximated by a Schottky junction, and the Fowler equation should be valid.

Figure 1 shows the square root of the quantum efficiency as a function of photon energy for the LCMO/STON junctions ($t=200$ nm). Satisfactory linear $R^{1/2}-h\nu$ relations are obtained for all of the samples, indicating the presence of a definite IB in the junction. With the increase in Ca content, the $R^{1/2}-h\nu$ slope decreases and the x -axis intercept of the $R^{1/2}-h\nu$ curve shifts to high energies. The former could be a consequence of the enhanced annihilation of the extra carriers with the increase in x and the latter is a signature of the growth of Φ_B . Two distinctive features can be identified from the data in Fig. 1. The first one is the monotonic increase in the barrier height with x and the second one is the considerable difference between the IBs of the two differently orientated junctions. From a first glance, the IB is higher in the (110) than in the (100) junctions. This is particularly obvious when the Ca content is low, and the typical $\Delta\Phi_B$ is ~ 0.1 eV, occurring for $x=0.1$. It could be a general feature of the manganite junctions noting the fact that similar phenomenon is observed in the LBMO/STON junctions as will be shown below. These results are different from those reported by Minohara *et al.*⁶

To get the further information on the effect of substrate orientation, in Fig. 2 we present the $R^{1/2}-h\nu$ relations for the (100) and (110) junctions with a constant hole content $x=0.33$ but different film thickness. An evolution of the orientation dependence with film thickness is evident. The difference in the IB is small in thin film junctions, and grows as t increases. Essentially the same behaviors are observed in LBMO/STON, though LBMO is different from LCMO in a

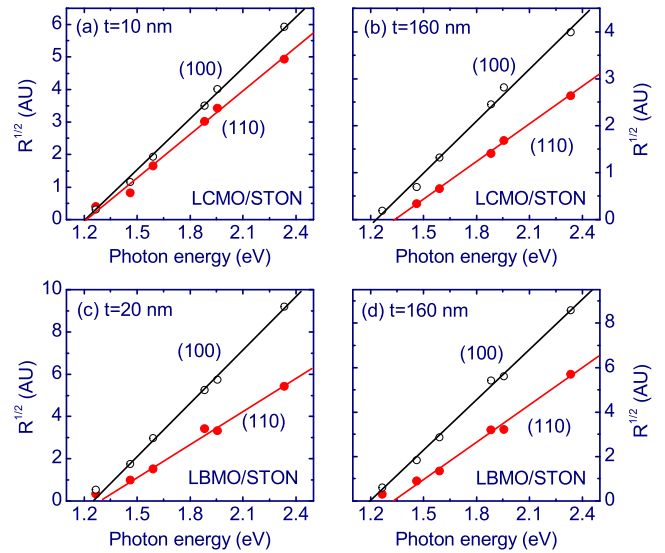


FIG. 2. (Color online) Square-root quantum efficiency as a function of photon energy for the (100) and (110)-orientated LCMO/STON and LBMO/STON junctions with different film thickness but a constant hole content of 0.33. Solid lines are fitting results.

sense that it has a different lattice strain. Figure 3(a) exemplifies the IB height as a function of Ca content for the LCMO/STON junctions. When Ca content is low, Φ_B is ~ 1.32 eV for the (110) junction and ~ 1.22 eV for the (100) junction. It keeps nearly constant with the increase in the Ca content until $x \sim 0.67$, above which a rapid growth occurs with further increasing x . Φ_B grows at different rates with t for the (100) and (110) junctions [Fig. 3(b)], which leads to the rapid growth of $\Delta\Phi_B$. It is worthwhile to note the correspondence between the Φ_B-t and $\Delta\Phi_B-t$ curves; $\Delta\Phi_B$ develops as Φ_B rises.

To get a clear picture of the effect of Ca content and film thickness on the IB, in Fig. 4 we present the $\Delta\Phi_B-x$ and the $\Delta\Phi_B-t$ relations for the LCMO/STON junctions. When film thickness is fixed to 200 nm, $\Delta\Phi_B$ shows a strong dependence on Ca content. It is ~ 0.1 eV when $x=0$, slightly decreases with x for $x < 0.67$, and falls swiftly with a further increase in x . In the case of $x=0.33$, $\Delta\Phi_B$ is small in thin film junctions, increases rapidly as t grows, and saturates at a value close to ~ 0.1 eV for $t > 80$ nm. These results clearly demonstrate the close relation between the orientation effect and the Ca content/film thickness.

The orientation effect observed here cannot be explained by the simple Schottky-Mott model, the latter proposes an

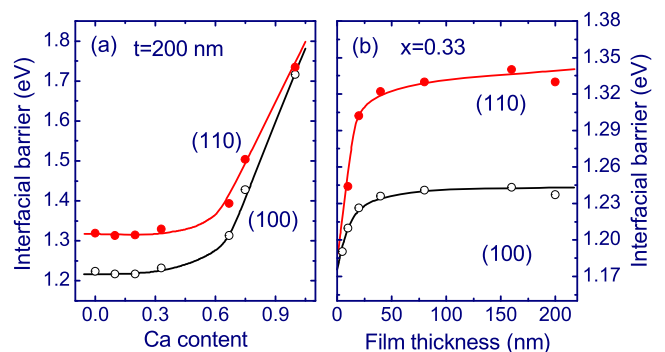


FIG. 3. (Color online) IB as a function of (a) the Ca content and (b) the thickness of the LCMO films. Solid lines are guides for the eye.

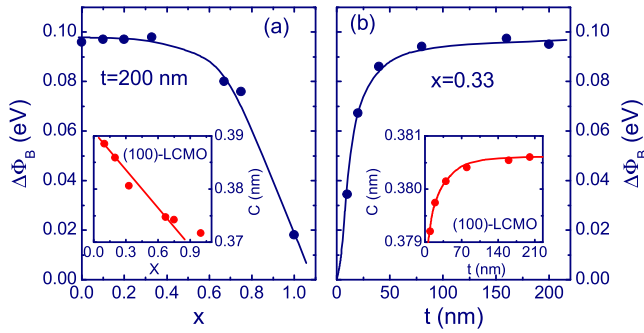


FIG. 4. (Color online) Difference of IB for the (110) and (100)-oriented LCMO/STON junctions. The $\Delta\Phi_B$ - x and Φ_B - t relations are, respectively, shown in [(a) and (b)]. The inset plots in [(a) and (b)] give the lattice constants as function of Ca content and film thickness, respectively. Solid lines are guides for the eye.

exclusive relation between the IB and the difference in the bulk work function of the metal and the bulk electron affinity of the semiconductor. The classical Fermi-level pinning mechanism based on the surface states of semiconductors does not account for the experiment results either. Because of the lattice mismatch between the films and the substrates, lattice stress in the former is expected to exist. As reported, lattice strains have a strong effect on IB, and a reduction in Φ_B up to 0.13 eV can be induced by tensile strains for the LCMO/STON junctions.⁴ This seems to suggest a higher IB in the (110) junctions since the (110) films are less strained than the (100) ones. However, the orientation effect observed here cannot be exclusively ascribed to lattice strains. As we know, the lattice stresses are tensile and compressive for the LCMO and LBMO films, respectively. This implies a reverse IB change for the two series of junctions, which is inconsistent with the experimental results.

To account for the buffer layer-induced change in the IB height of the $\text{La}_{0.7}\text{Sr}_{0.3}\text{MnO}_3/\text{SrMnO}_3/\text{STON}$ junctions, a model of interface dipole has been proposed by considering the polarity mismatch at the interface.⁸ When net interface charges exist, a polar discontinuity at the interface occurs. According to Hikita *et al.*, in this case extra charges due to a screening effect will appear to avoid a diverging electrostatic potential arising from the interface, yielding an effect on the IB. It was found that IB height grew by as high as ~ 0.5 eV while the SrMnO_3 coverage increased from 0 to 1.

In a similar picture, the present experiment results can be qualitatively understood. Noting that the terminal layer of the (100) SrTiO_3 is either TiO_2 or SrO , the interface will be $\text{MnO}_2/\text{La}_{1-x}\text{Ca}_x\text{O}/\text{TiO}_2$ or $\text{La}_{1-x}\text{Ca}_x\text{O}/\text{MnO}_2/\text{SrO}$, with a sheet charge density of $-(1-x)q/(+4q)/0$ or $+(1-x)q/-(1-x)q/0$, where q is the electron charge. Assuming the same population of the two terminal layers at the interface, the net effect of charge screening on IB will be negligibly small. In contrast, for the (110) SrTiO_3 , there are two terminal layers with the formulae of SrTiO and O_2 , respectively. The corresponding interfacial atomic structures will be $\text{La}_{1-x}\text{Ca}_x\text{MnO}/\text{O}_2/\text{SrTiO}$ and $\text{O}_2/\text{La}_{1-x}\text{Ca}_x\text{MnO}/\text{O}_2$, with the respective sheet charge densities of $+4q/-4q/+4q$ and $-4q/+4q/-4q$. Considering the absence of cations, significant oxygen depleting is expected for the O_2 -terminated layer, and the actual sheet charge distribution could be

$-4q/+4q/-4(1-\delta)q$, where δ is the content of oxygen vacancies on the terminal layer of the substrate. To screen the effect of the interface polarity mismatch, $-2\delta q$ extra charge will be required. As a result, the IB of the (110) junctions is enhanced. A rough estimation, referencing the result of Hikita *et al.*, shows that to get a $\Delta\Phi_B$ of ~ 0.1 eV, the δ value will be ~ 0.07 assuming the population of the O_2 -layer of 1/2 at the (110) interface, that is, minor oxygen deflation can yield sizable effects.

In the presence of oxygen deficiency, the interface structure becomes $\text{La}_{1-x}\text{Ca}_x\text{MnO}_{(1-\delta')}/\text{O}_{2(1-\delta)}/\text{SrTiO}$ and $\text{O}_{2(1-\delta')}/\text{La}_{1-x}\text{Ca}_x\text{MnO}_{(1-\delta')}/\text{O}_{2(1-\delta)}$, where δ' is the content of oxygen vacancies. In this case, a reduced $\Delta\Phi_B$ is expected because of the decrease in the extra charge to screen the polarity mismatch [$-2\delta q \rightarrow -2(\delta-\delta')q$]. This may explain the decrease in $\Delta\Phi_B$ above $x=0.67$. In fact, the x-ray diffraction analysis performed for the LCMO films has revealed a deviation of the c - x relation from linearity above $x=0.67$ [inset in Fig. 4(a)], indicating the oxygen non-stoichiometry in the films, where c is the out-of-plane lattice constant. As for the thickness dependence of $\Delta\Phi_B$, it may also stem from the oxygen deflation in the films. The $\Delta\Phi_B$ - t relation mimics the c - t curve [inset in Fig. 4(b)], probably a signature of the simultaneous occurrence of oxygen losing and structure defects.

Development of the IB as film thickness grows has been studied by Minohara *et al.* for the (100) and (110)-oriented $\text{La}_{0.6}\text{Sr}_{0.4}\text{MnO}_3/\text{STON}$ junctions.⁶ Different from the present results, Φ_B is found to be higher in the (100) junction than in the (110) junction. The substrates employed by Minohara *et al.* have been treated at a temperature as high as 1050 °C in high vacuum. This may lead to, in addition to oxygen depleting, considerable aggregation of Nb atoms on substrate surface. This process could be different for the (100) and (110) substrates due to their different terminal structures. In contrast, as-polished STON substrates have been used in our experiments, which explain the different orientation effects.

This work has been supported by the National Basic Research of China, the National Natural Science Foundation of China, the Knowledge Innovation Project of the Chinese Academy of Science, and the Beijing Municipal Nature Science Foundation.

¹M. Sugiura, K. Urugou, M. Noda, M. Tachiki, and T. Kobayashi, *Jpn. J. Appl. Phys.*, Part 1 **38**, 2675 (1999); H. Tanaka, J. Zhang, and T. Kawai, *Phys. Rev. Lett.* **88**, 027204 (2001).

²J. R. Sun, C. M. Xiong, T. Y. Zhao, S. Y. Zhang, Y. F. Chen, and B. G. Shen, *Appl. Phys. Lett.* **84**, 1528 (2004); N. Nakagawa, M. Asai, Y. Mukunoki, T. Susaki, and H. Y. Hwang, *ibid.* **86**, 082504 (2005).

³J. R. Sun, B. G. Shen, Z. G. Sheng, and Y. P. Sun, *Appl. Phys. Lett.* **85**, 3375 (2004); Z. G. Sheng, B. C. Zhao, W. H. Song, Y. P. Sun, J. R. Sun, and B. G. Shen, *ibid.* **87**, 242501 (2005).

⁴W. M. Lü, A. D. Wei, J. R. Sun, Y. Z. Chen, and B. G. Shen, *Appl. Phys. Lett.* **94**, 082506 (2009).

⁵A. D. Wei, J. R. Sun, W. M. Lv, and B. G. Shen, *Appl. Phys. Lett.* **95**, 052502 (2009).

⁶M. Minohara, Y. Furukawa, R. Yasuhara, H. Kumigashira, and M. Oshima, *Appl. Phys. Lett.* **94**, 242106 (2009).

⁷R. H. Fowler, *Phys. Rev.* **38**, 45 (1931).

⁸Y. Hikita, M. Nishikawa, T. Yajima, and H. Y. Hwang, *Phys. Rev. B* **79**, 073101 (2009).